MATHEMATICAL MODELLING OF HEAVY-ORE LOAD TRAIN EQUIPPED WITH ELECTRONICALLY CONTROL PNEUMATIC BRAKE

S-C Wang and X. Xia

Department of Electrical, Electronic and Computer Engineering, University of Pretoria, Pretoria, 0002, South Africa, e-mail: jscwang@tuks.co.za

Abstract: The purpose of this paper is to derive suitable models for the design of controller for the heavy-ore load train system that is equipped with the newest railway brake system—the electronically control pneumatic brake (ECPB). Special train models are then obtained by simplifying the general one under different track conditions such as straight-flat, curving-flat and straight-slope, etc. A distinction is also made between known and unknown track information (say, provided by global positioning system - GPS).

Keywords: electronically control pneumatic brake, global positioning system

1. INTRODUCTION

Mineral exports had been a large source of income for the South Africa, and the railway system has been proven to be the most efficient way of transporting the heavy loads. Coallink is a Spoornet specialist business unit that provides world-class transportation of South Africa's export coal, from the Mpumalanga coal fields to the Richards Bay Coal Terminal by train.

Since late 1990's the Coallink system has reached it maximum capacity due to the increase in demand. Both the train lengths (200 wagons that stretch 2.5 kilometers) as well as the wagon size (from small to jumbo) have reached the maximum allowed by specification of the narrow-gauge system. Various upgrades on the trains are now being considered to reduce the trip time as well as the operational cost. Currently an upgrade is in process from the old pneumatic control brake system developed by George Westinghouse in 1869 to the new Electronically Controlled Pneumatic Brakes (ECPB) system installed on the wagons.

The ECPB system replaces the pneumatic control signals (air pressure differential in the brake pipe) with electronic signals. This results in faster response times and an spontaneous braking across the whole train can be achieved (air signal can only travel at speed of the sound). The ECPB brake system has been studied by Chen *et al.* (1998) which has shown to provide improvement in braking performance, including fuel savings, brake shoe wear reduction, the quick response time of the brake, etc. One problem still remaining is to determine the new model that facilitates the cruise controller design for the freight train system that is equipped with ECPB. Currently the control system is based on model of the train that equipped with the pneumatic control pneumatic braking system; and track condition is based on the experience of train operator therefore a new model is needed to enable an optimal design for the controller and correct operation of the trains equipped with the ECPB and, possibly, GPS signals.

2. GOVERNING EQUATIONS OF HEAVY-ORE TRAIN

In the operation of the freight train the operation of the pneumatic brake system is critical because it provides the retarding force (F_r) to the train to ensure the safety operation of the freight train. The behaviour of the pneumatic brake system can be described as linear model such that the retarding force of a pneumatic brake system is a function of the brake cylinder pressure P_i (Blaine *et al.*, 1979) as

$$F_r = P_i * A \cdot L \cdot f_s \cdot e_b \tag{1}$$

where A is the cross section area of the brake cylinder; L is the lever ratio, e_b is the efficiency of the brake and f_s is the friction coefficient of the brake shoe which is a nonlinear function depending on the speed of the freight train as in figure 1.

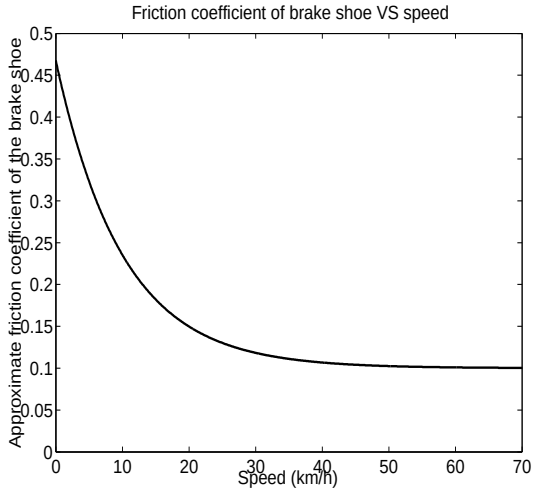

Fig. 1. The characteristic of the friction coefficient of the brake shoe verse speed

The main difference between the ECPB and the traditional air signal pneumatic brake is that simultaneous application of the brake force on the wheels can be achieved in the case of the ECPB, and long delay is expected for air signal when the freight train is 2.5 kilometer long.
The running resistance $\mathbf{R}$ of the train consists of aerodynamic drag $\mathbf{R^a}$ and rolling mechanical resistance $\mathbf{R^r}$ which is commonly expressed as

$$\mathbf{R} = \underbrace{C_0 + C_\nu \nu}_{\mathbf{R^r}} + \underbrace{C_a \nu^2}_{\mathbf{R^a}} \tag{2}$$

Where ν is the velocity of the wagons or locomotive and the coefficient C_0, C_ν and C_a are obtained by wind tunnel tests (Chen and Zhang, 1998; Suzuki *et al.*, 2003). The aerodynamic drag is composed of two components: (1) the form drag arising from the pressure distribution along the nose and the tail of the train, and (2) the skin friction drag over the entire surfaces of the train. The aerodynamic drag will be the dominant resistance, especially in the high speed range. The rolling resistance, which comes from the friction between wheel and rail, is dominant in the low speed range (Komandi, 1999; Popv *et al.*, 2002).

In the longitudinal motion of the freight train, couplers play an important role in connecting the adjacent wagons or locomotives together and pass on the traction force generated by the locomotive in the axial direction. The coupler can be described by a spring model such that the restoring force F_c of a coupler is a function of the relative displacement Δx between two adjacent wagons as

$$f(\Delta x) = k^- \Delta x \tag{3}$$

where k^- is the stiffness coefficient. for an ideal spring, k^- is a constant; however, for a coupler used in the freight train, k^- usually depends on the displacement Δx non-linearly.

The locomotive and wagons dynamic motion can be described in three displacement motions (longitudinal, lateral and vertical) and three rotations motions (yaw, pitch and rolling) in six degrees of freedom as

$$\begin{aligned}
M_{(i)}\ddot{x}_i &= F_{cH(i)} - F_{cH(i+1)} + F_{AFH(i)} + F_{ARH(i)} \\
M_{(i)}\ddot{y}_i &= F_{cL(i)} + F_{cL(i+1)} + F_{AFL(i)} + F_{ARL(i)} \\
M_{(i)}\ddot{z}_i &= F_{cV(i)} - F_{cV(i+1)} + F_{AFV(i)} + F_{ARV(i)} + M_{(i)} \cdot g \\
Jx_{(i)}\ddot{\phi}_{(i)} &= L_{BS(i)}(F_{AVL(i)} - F_{AVR(i)}) + L_{HGC(i)}(M_{(i)}\ddot{Y}_{(i)}) \\
Jy_{(i)}\ddot{\theta}_{(i)} &= (F_{cH(i)} - F_{cH(i+1)})(L_{HGC(i)} - 0.5L_{c(i)}\theta_i) + (F_{AFH(i)} + F_{ARH(i)})L_{HGC(i)} + (F_{cV(i)} - F_{cV(i+1)}) \cdot L_{cFR(i)} + (F_{AFV(i)} - F_{ARV(i)}) \cdot L_{FR(i)} \\
Jz_{(i)}\ddot{\psi}_{(i)} &= -0.5L_{cFR(i)}(F_{cH(i)} + F_{cH(i+1)})\psi_{(i)} + 0.5L_{cFR(i)}(F_{cL(i)} + F_{cL(i+1)}) + 0.5L_{FR(i)}(F_{ALF(i)} - F_{ALR(i)})
\end{aligned} \tag{4}$$

where

$M_{(i)}$	Mass of the i_{th} car (kg),
$Jx_{(i)}$	Roll moments of inertia of i_{th} car (kg.m^2),
$Jy_{(i)}$	Pitch moments of inertia of i_{th} car (kg.m^2),
$Jz_{(i)}$	Yaw moments of inertia of i_{th} car (kg.m^2),

$L_{FR(i)}$	Distance between front and rear centerplates of i_{th} car (m),
$L_{cFR(i)}$	Distance between front and rear coupler pins in i_{th} car body (m),
$L_{BS(i)}$	Half distance between left and right bolster spring centers of the i_{th} car (m),
$L_{HGC(i)}$	The height of the centroid of i_{th} car body above coupler Gravitational accelerations (m/s^2),
X_i	Longitudinal displacement of centroid of car body relative to the starting station (m),
R	Running resistance.
Y_i	Lateral displacement of centroid of car body relative to railway center line (m),
Z_i	Vertical displacement of the centroid of car body relative to track plane (m),
$\phi_{(i)}$	Roll displacement of i_{th} car body (radian,)
$\theta_{(i)}$	Pitch displacement of i_{th} car body (radian),
$\psi_{(i)}$	Yaw displacement of i_{th} car body (radian),
$F_{cL(i)}$,$F_{cL(i+1)}$	Lateral components of front or rear coupler forces for the i_{th} car (N),
$F_{cV(i)}$,$F_{cV(i+1)}$	Vertical components of front or rear coupler forces for the i_{th} car (N),
$F_{cH(i)}$,$F_{cH(i+1)}$	Longitudinal components of front or rear coupler forces for the i_{th} car (N),
$F_{AFH(i)}$,$F_{ARH(i)}$	Longitudinal force acting on the i_{th} car body by front or rear car thought the centerplate (N),
$F_{AFL(i)}$,$F_{ARL(i)}$	Lateral force acting on the i_{th} car body thought front and rear centerplate by front and rear car respectively (N),
$F_{AFV(i)}$,$F_{ARV(i)}$	Vertical force acting on the i_{th} car body by front or rear car thought front and rear bolster spring (N),
$F_{AVL(i)}$,$F_{AVR(i)}$	Vertical force acting on the i_{th} car body by the two car thought left and right bolster springs (N).

The motion coordinates proposed by Li *et al.* (1989) and Garg and Dukkipati (1984) are shown in figure 2. It has been observed by Garg and Dukkipati (1984) that a relatively weak coupling exists between the vertical and lateral motion of a vehicle and, therefore, that it may not be necessary to include the vertical degrees of freedom in the study of the lateral response of the vehicle or the lateral degrees in the vertical response, etc.

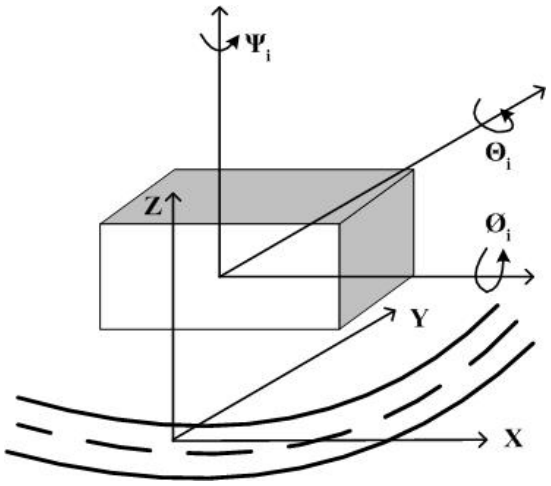

Fig. 2. Coordinates for the freight train

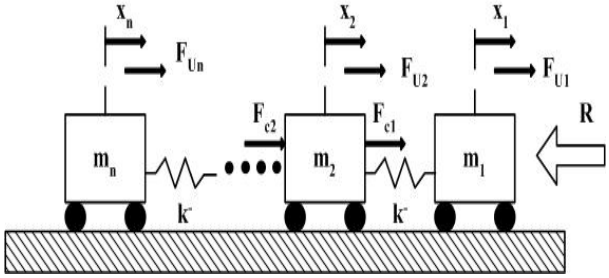

Fig. 3. Longitudinal force diagram of the freight train

For the case of the flat straight rail track the Longitudinal force diagram of the freight train is shown in figure 3 there the dynamic equation of the i_{th} wagon or locomotive within the train can be written by using Newton's second law ($\sum Force = mass \cdot acceleration$) suggested by Yang and Sun (2002) as

$$\begin{aligned} m_1\ddot{x}_1 &= F_{U1} + k^-(x_1 - x_2) - R_1^r m_1 - \\ &\quad R^a \sum_{i=1}^{n} m_i \\ m_i\ddot{x}_i &= F_{Ui} - k^-(x_i - x_{i-1}) - k^-(x_i - \\ &\quad x_{i+1}) - R_i^r m_i \\ m_i\ddot{x}_n &= F_{Un} - k^-(x_n - x_{n-1}) - R_n^r m_n \\ i &= 2, \ldots, n-1 \end{aligned} \tag{5}$$

where F_{Ui} can be the traction force F_A or the retarding force F_r provided by the locomotive and retarding force for the wagons only; x_i and $\dot{x}_i$ represent the position and velocity of the i_{th} cars. The retarding force provided by the locomotive is normally different from equation (1) as suggested by the Blaine *et al.* (1979) because the locomotive is equipped with an additional dynamic brake.

For the current model of the train operation the track conditions are interpreted by the train operator, then the change is made. But now with the help of GPS that provides the longitude and latitude coordinates of the train position, the track conditions can then be interpreted by model to automatically make the change. Like in the case of the curving track shown in figure 2 where each car passes by the different position on the curved track, say the curve radius of the track is being provided by the global positioning system (GPS), then it is necessary to look at the longitudinal and lateral displacement motion of the freight train .The longitudinal dynamic motion of the freight train on the curving track will be given as

$$\begin{aligned} m_1\ddot{x}_1 &= (F_{U1} + k^-(x_1 - x_2) - R_1^r m_1 - \\ &\quad R^a \sum_{i=1}^{n} m_i) \cos\psi_1 \\ m_i\ddot{x}_i &= (F_{Ui} - k^-(x_i - x_{i-1}) - k^-(x_i - \\ &\quad x_{i+1}) - R_i^r m_i) \cos\psi_i \\ m_i\ddot{x}_n &= (F_{Un} - k^-(x_n - x_{n-1}) - R_n^r m_n) \\ &\quad \cos\psi_n \\ i &= 2, \ldots, n-1 \end{aligned} \tag{6}$$

and lateral dynamic motion will be given as

$$\begin{aligned} m_1\ddot{y}_1 &= (F_{U1} + k^-(y_1 - y_2) - R_1^r m_1 - \\ &\quad R^a \sum_{i=1}^{n} m_i) \sin\psi_1 \\ m_i\ddot{y}_i &= (F_{Ui} - k^-(y_i - y_{i-1}) - k^-(y_i - \\ &\quad y_{i+1}) - R_i^r m_i) \sin\psi_i \\ m_i\ddot{y}_n &= (F_{Un} - k^-(y_n - y_{n-1}) - R_n^r m_n) \\ &\quad \sin\psi_n \\ i &= 2, \ldots, n-1 \end{aligned} \tag{7}$$

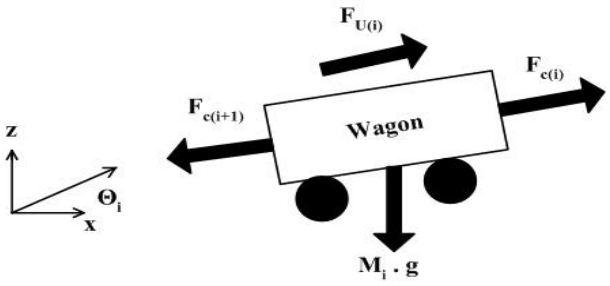

Fig. 4. Longitudinal force diagram of the freight train on inclined track

In the case of the straight incline or decline track shown in figure 4 each car will move along the incline track at an angle Θ_i, say the elevation angle of the track is being provided by the global positioning system (GPS), then it is necessary to look at the longitudinal and vertical displacement motion of the freight train .The longitudinal dynamic motion of the freight train on the inclined track will be given as

$$\begin{aligned} m_1\ddot{x}_1 &= (F_{U1} + k^-(x_1 - x_2) - R_1^r m_1 - \\ &\quad R^a \sum_{i=1}^{n} m_i) \cos\theta_1 \\ m_i\ddot{x}_i &= (F_{Ui} - k^-(x_i - x_{i-1}) - k^-(x_i - \\ &\quad x_{i+1}) - R_i^r m_i) \cos\theta_i \\ m_i\ddot{x}_n &= (F_{Un} - k^-(x_n - x_{n-1}) - R_n^r m_n) \\ &\quad \cos\theta_n \\ i &= 2, \ldots, n-1 \end{aligned} \tag{8}$$

and vertical dynamic motion will be given as

$$\begin{aligned} m_1\ddot{z}_1 &= (F_{U1} + k^-(z_1 - z_2) - R_1^r m_1 - \\ &\quad R^a \sum_{i=1}^{n} m_i) \sin\theta_1 + m_1 \cdot g \\ m_i\ddot{z}_i &= (F_{Ui} - k^-(z_i - z_{i-1}) - k^-(z_i - \\ &\quad z_{i+1}) - R_i^r m_i) \sin\theta_i + m_i \cdot g \\ m_i\ddot{z}_n &= (F_{Un} - k^-(z_n - z_{n-1}) - R_n^r m_n) \\ &\quad \sin\theta_n + m_n \cdot g \\ i &= 2, \ldots, n-1 \end{aligned} \tag{9}$$

where g is the gravitational acceleration.

3. SIMULATION

In this section the simulation on longitudinal motion of equation (5) of the train that consists of a lead locomotive and 3 wagons has been set up and it is assumed that the train is started at the equilibrium state of moving at constant velocity of 30km/h. The operation status of the cars, like the displacement and velocity of each car within the train under different input force (traction or retarding force) are being monitored. The locomotive and wagon parameters are in table 1, and the rolling resistance and aerodynamic resistance coefficients (obtained from the experiment done on the Japan SHINKANSEN high speed train (HST)) are shown in table 2.

Table 1. Parameters of the freight train

Locomotive mass	113126kg
Locomotive Max speed	100km/h
Max Loco. braking effort	2187kN
Wagon loaded mass	104250kg
Wagon empty mass	20250kg
Wagon brake force	94.6kN
Coupler coefficient (k^-)	80kN/m

Table 2. Other parameters for the train system

Rolling coefficient C_0	1.1766X10^{-2}N/kg
Rolling coefficient C_ν	7.7616X10^{-4}N·s/m·kg
Aerodynamic coefficient C_a	1.6X10^{-5}N·s^2/m^{2}kg

The input longitudinal force has been chosen as in figure 5 where locomotive will provide a step traction force at t=10 and t=21, and the step brake force will be apply at t=20 for a second.

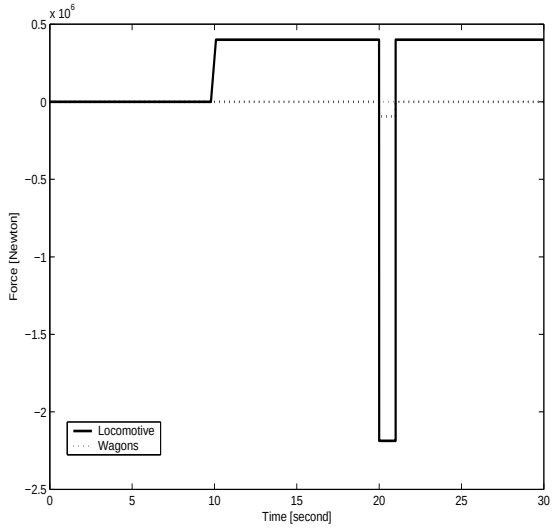

Fig. 5. Time diagram of the input force on the train system

As can be see from figure 6 and 7 the velocity of the train starts at equilibrium of 8.33m/s (or 30km/h) and the velocity has been increased and propagated thought the train as the traction force propagated from the locomotive till the last wagon. When the brake force is applied at t=21 a dramatic decrease can be seen in velocity when all the brake has been applied for a second. It can also be observed that the oscillation effects on the displacement and velocity are caused by the coupler acting on each car.

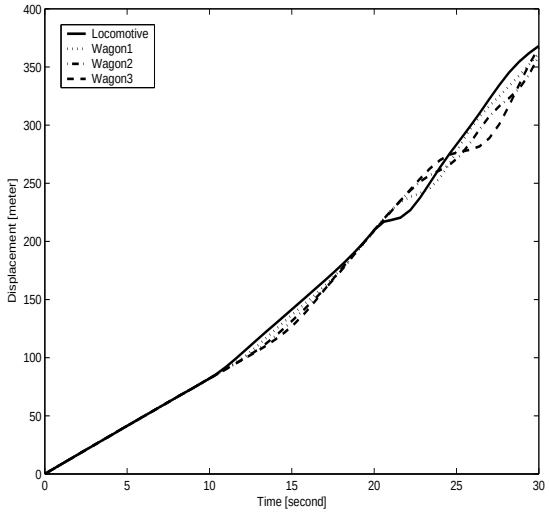

Fig. 6. time diagram of the displacement of the train system

4. CONCLUSION

In the problem of finding the models for the freight train system equipped with ECPB, several important characteristics regarding the ECPB brake system have been pointed out and parameters within the brake have been identified. A general dynamical model of six degrees of freedom has been derived. Special train models are also given under different track conditions. Preliminary simulation results are demonstrated to show that the model developed under the straight-flat track condition reflect to an extend the operation of the train. Further detailed developments, simulation as well as testing are currently under investigation.

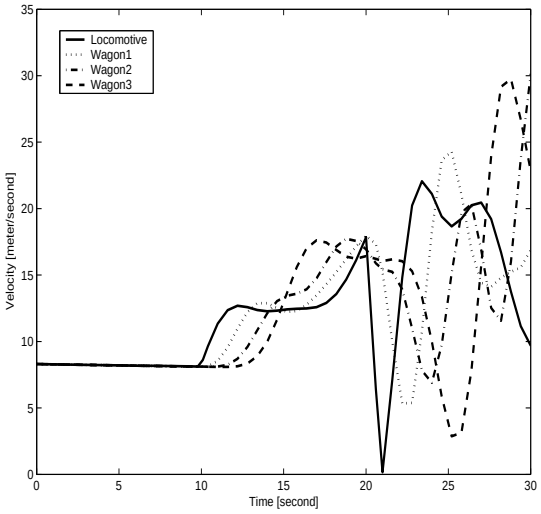

Fig. 7. Time diagram of the velocity of the train system

REFERENCES

Blaine, D.G., C.W. Parker, D.F. Dilgard, F.R. Ellis and R.E. Winter (1979). Engineering and design of railway brake systems. Air Brake Association.

Chen, E-D., Y.H. Tse, F. Larry and L.F. Myers (1998). Economic considerations of operating a train with electronically controlled pneumatic (ecp) brakes. In: *Proceeding of the 1998 ASME/IEEE Joint*. pp. 9–19.

Chen, N. and J. Zhang (1998). Experimental investigation on aerodynamic drag of high speed train. *Journal of the china railway socity* (20), 40–46.

Garg, V.K. and R.V. Dukkipati (1984). *Dynamics of railway vehicle systems*.

Komandi, G. (1999). An evaluation of the concept of rolling resistance. *Journal of Terramechanics* **36**, 159–166.

Li, Z., Y. Zheng and X. Qiu (1989). Operation simulator of heavy haul train, 1989. main line railway electrification. *Main Line Railway Electrification* pp. 351–355.

Popv, V.L., S.G. Psakhie, E.V. Shilko, A.I. Dmitruev, K. Knothe, F. Bucher and M. Ertz (2002). Friction coefficient in "rail-wheel"-contacts as function of material and loading parameters. *Physical Mesomechanics* **5**(3), 17–24.

Suzuki, M., K. Tanemoto and T. Maeda (2003). Aerodynamic characteristic of train/vehicles under cross winds. *Journal of Wind Engineering and Industrial Aerodynamics* (91), 209–218.

Yang, C-D and Y-P Sun (2002). Mixed h /h2 cruise controller design for high speed train. *International Journal of Control* **72**(9), 905–920.